Chimpanzee High-Resolution Minimum Deformation Average and Application To Aging and Sex Differences

#1953

Gabriel A. Devenyi[1,2](gabriel.devenyi@mcgill.ca), Chet Sherwood[4], William D. Hopkins[5], Armin Raznahan[6] and M. Mallar Chakravarty[1,2,3]

[1]Cerebral Imaging Center, Douglas Mental Health University Institute, Montreal, Canada. [2]Department of Psychiatry, McGill University, Montreal, Canada. [3]Department of Biomedical Engineering, McGill University, Montreal, Canada. [4]Department of Anthropology and Center for the Advanced Study of Human Paleobiology, The George Washington University, Washington, DC 20052. [5]Department of Comparative Medicine, University of Texas MD Anderson Cancer Center, Bastrop, TX, 78602 [6]Developmental Neurogenomics Unit, Human Genetics Branch, National Institute of Mental Health, Bethesda, MD, 20892, USA

Introduction

- A key question in the evolutionary change of brain structures across the phylogeny is to determine how developmental trajectory and sex-specific anatomy differ across primates[1].
- Understanding these key differences may help elucidate the relationship between highly plastic and variable regions in humans and the hypothesis that these regions emerge more recently during evolution.
- We address these outstanding questions using data from our closest living genetic relative, the Chimpanzee (Pan troglodytes). Using structural neuroimaging of the Chimpanzee, we examine developmental trajectory, sexual differentiation, and variability of brain structure using a deformation based morphometry approach.
- A minimum deformation average was constructed to visualize the average anatomy, and the resulting deformation fields were used to compute subject-wise differences in local volume.

Data

- We obtained raw DICOM data of 261 T1-weighted MRIs of 216 individuals (87 M, 129 F) ages 6 to 53 from the National Chimpanzee Brain Resource, along with basic demographic information of age and sex at date of each scan.
- Scans were collected on a large variety of scanners, at numerous sites, with varying resolution (voxel dimensions 0.3 -- 1.2 mm) and TR/TEs, 139 at 1.5 T and 77 at ~3 T.

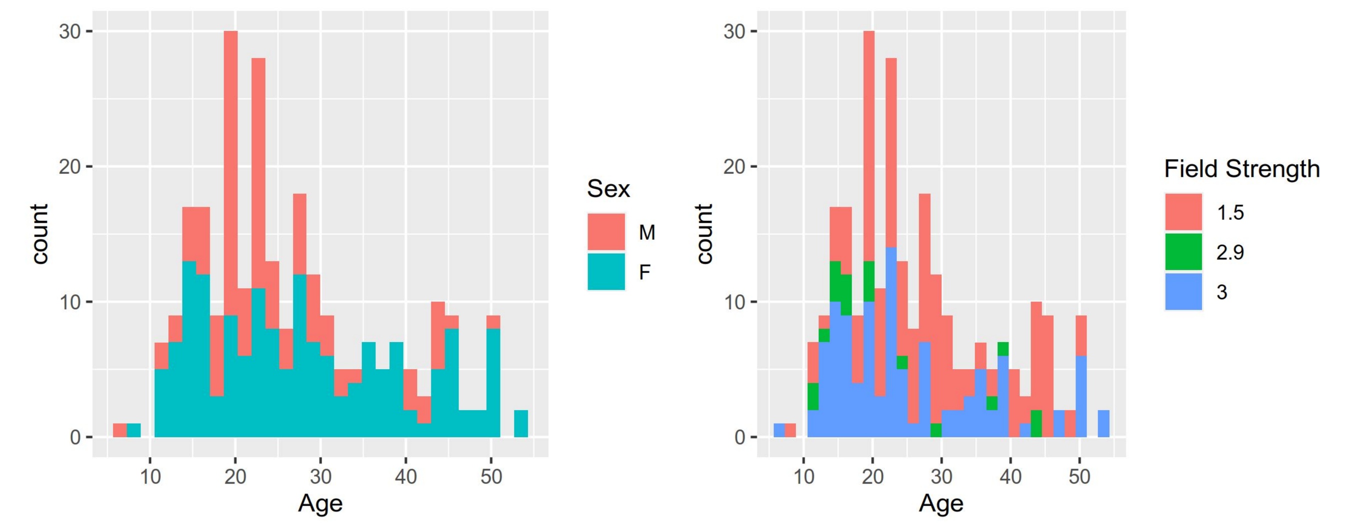

Figure 1: Sex/age, and Field Strength/age distribution of MRI scans included during template construction.

Methods

- Raw DICOMs were converted to MINC2 and pre-registered rigidly to the MNI ICBM 09c symmetric model.
- Scans were preprocessed using an iterative implementation of the ITKN4 algorithm, where a brain mask and tissue classification was estimated along with the bias field correction using the MNI ICBM 09c priors.
- Scans were extracted and flipped left-right to produce 432 scans, were averaged, upsampled to 0.4 mm^3 and used as the starting target for `antsMultivariateTemplateConstruction2.sh`[2] to produce an symmetric unbiased average of the population.
- Brain masks and classifications were then transformed into the average population space and combined to produce a new set of priors. First-round priors were then used to re-preprocess the raw scans, and another round of model construction was used to produce a final symmetric population average as brain mask, and classification probabilities.

The affine transforms and nonlinear deformation fields from template construction were then post processed to produce two forms of voxel-wise Jacobians:

- Relative -- each subject-wise warp field is post-processed along with brain mask to estimate any residual affine components which are then subtracted from its Jacobian to produce a pure relative Jacobian map
- Absolute -- the determinant of each affine transform is calculated and its value is added to the warp field to produce an absolute Jacobian map

After computation of the Jacobians they were smoothed with a 3D Gaussian with FWHM of 1.2 mm.

Statistics

Total brain volume, volume of GM, WM and CSF were modelled in R/3.6.3 using lme4/1.1-23 and lmerTest/3.1-2. Voxel-wise linear models for both absolute and relative Jacobians were modelled in R/3.6.3 using RMINC/1.5.2.2 with mixed effect linear models, with fixed effects of sex, second order natural spline of age, and random intercept effect of subject and MRI field strength. Multiple comparisons were corrected for using false discovery rate (FDR) with degrees of freedom estimated with Satterthwaite's approximation and thresholded at 5%. Subjects were weighted in lmer models using the contrast-to-noise ratio (CNR) of the scan.

Results

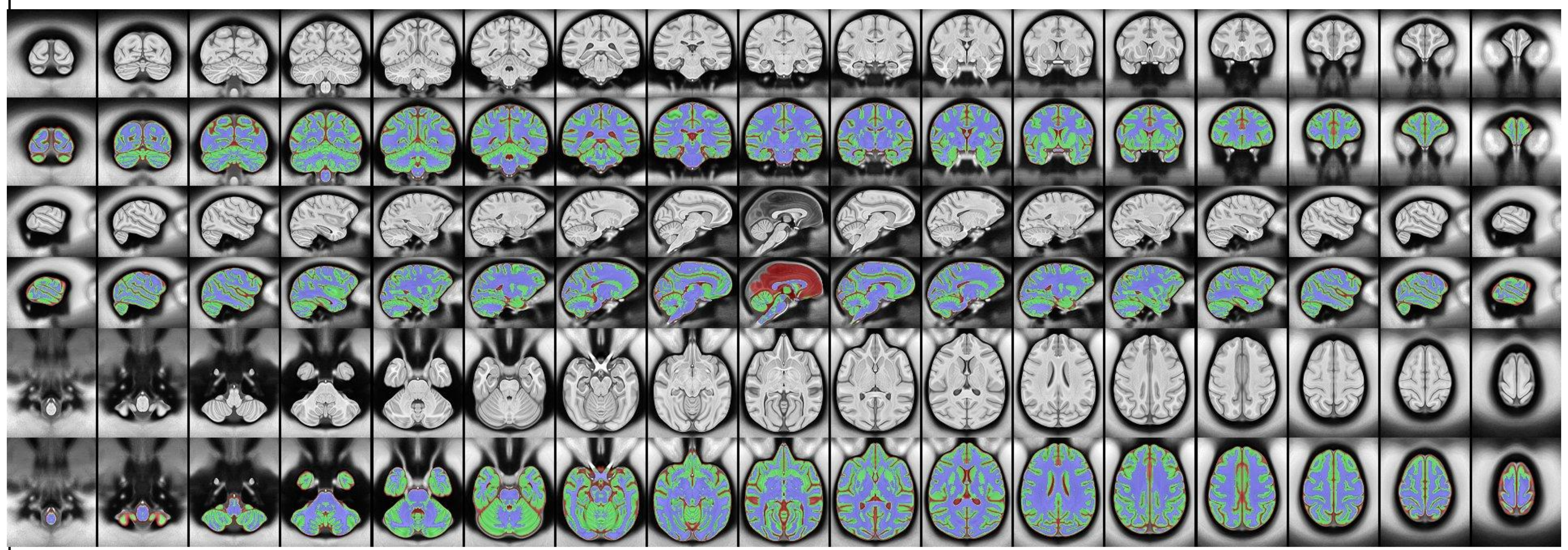

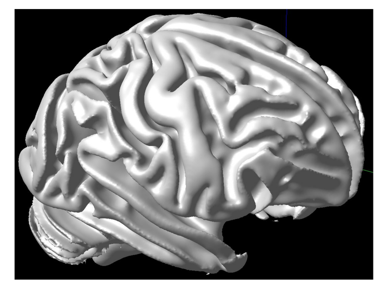

Figure 2: Representative slices of the minimum deformation average of the chimpanzee, with consensus CSF/GM/WM segmentation (left). The full field of view model (below), and cortex surface (left).

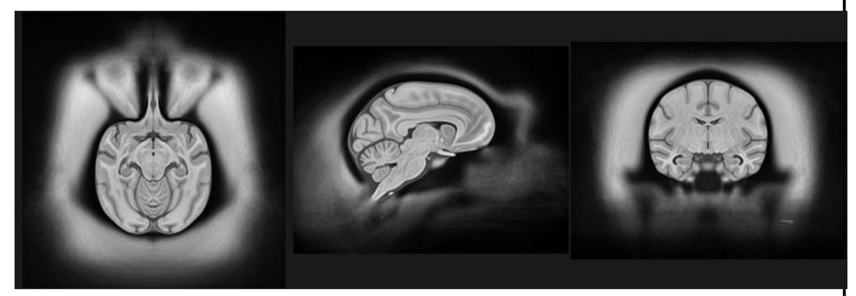

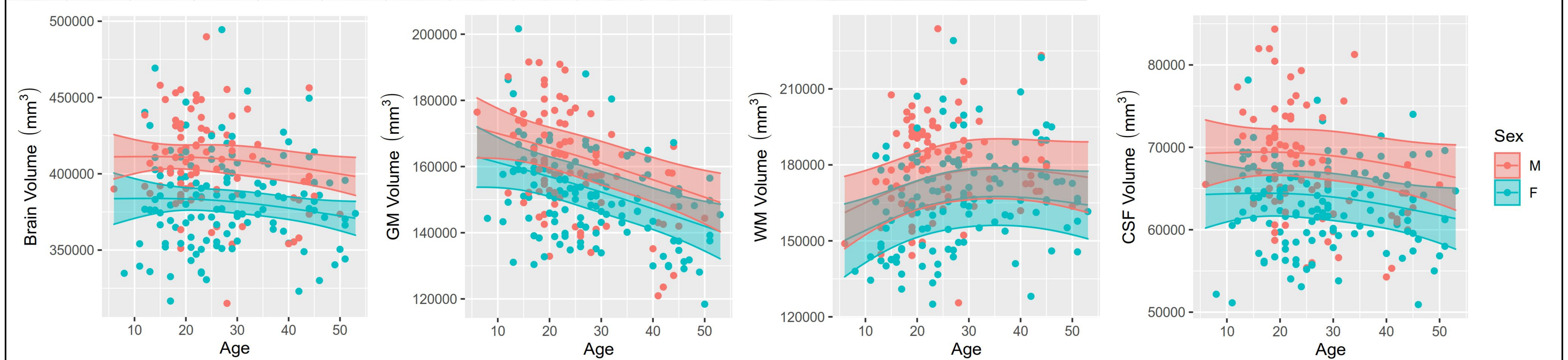

Figure 3: Whole brain, gray matter (GM), white matter (WM), and cerebral spinal fluid (CSF) volumes over the chimpanzee lifespan, split by sex and modelled with a second order natural spline.

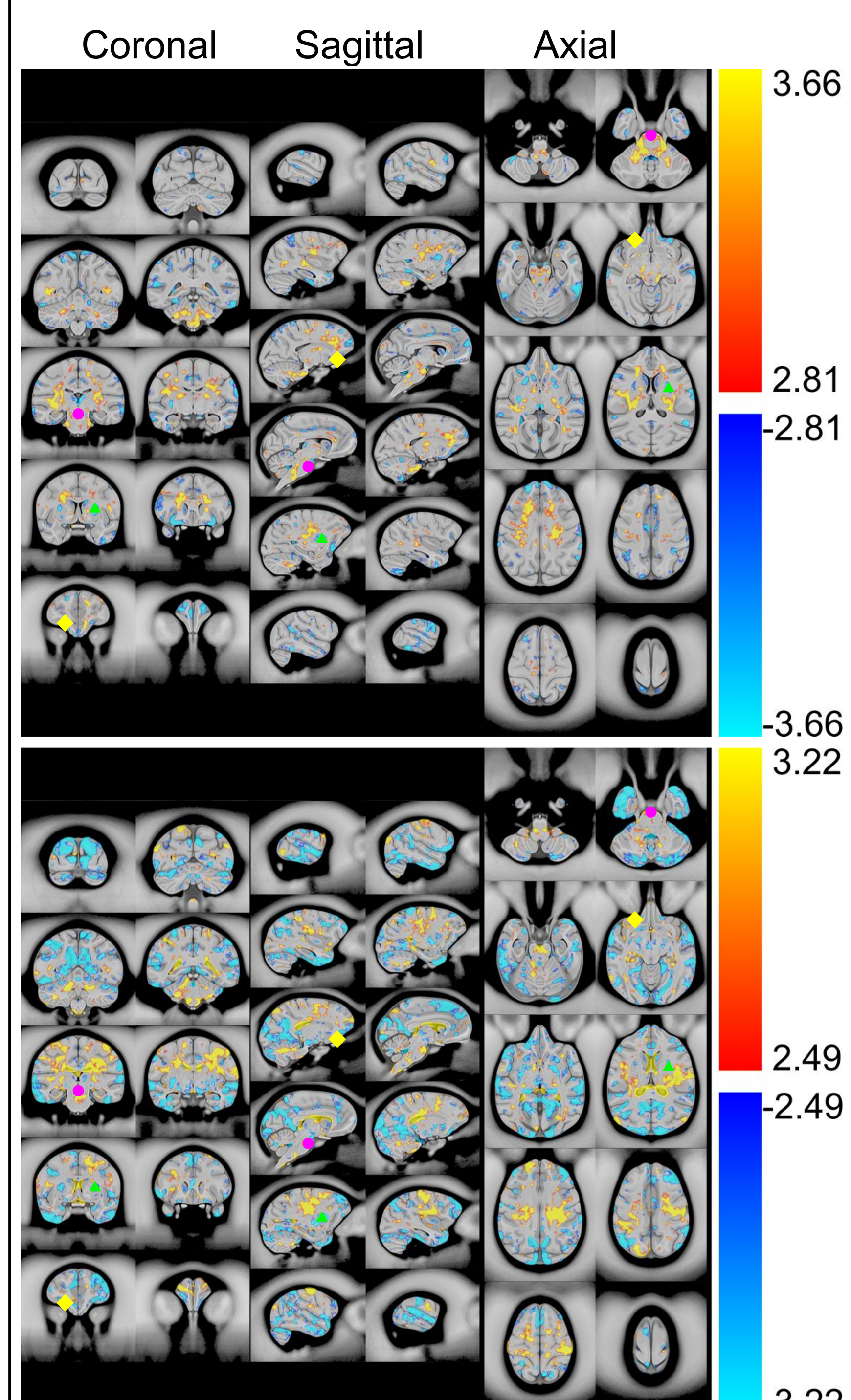

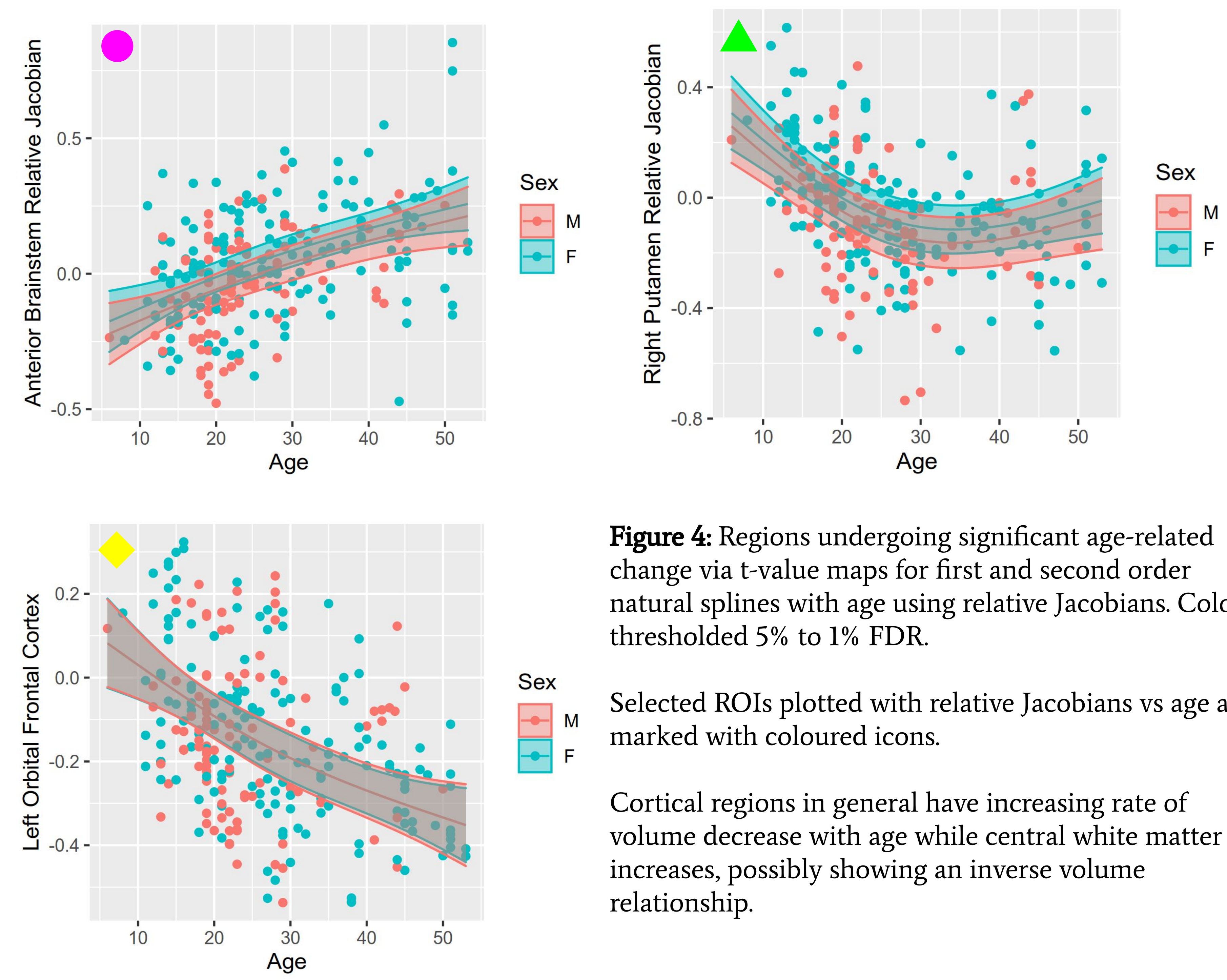

Figure 4: Regions undergoing significant age-related change via t-value maps for first and second order natural splines with age using relative Jacobians. Colour thresholded 5% to 1% FDR.

Selected ROIs plotted with relative Jacobians vs age and marked with coloured icons.

Cortical regions in general have increasing rate of volume decrease with age while central white matter increases, possibly showing an inverse volume relationship.

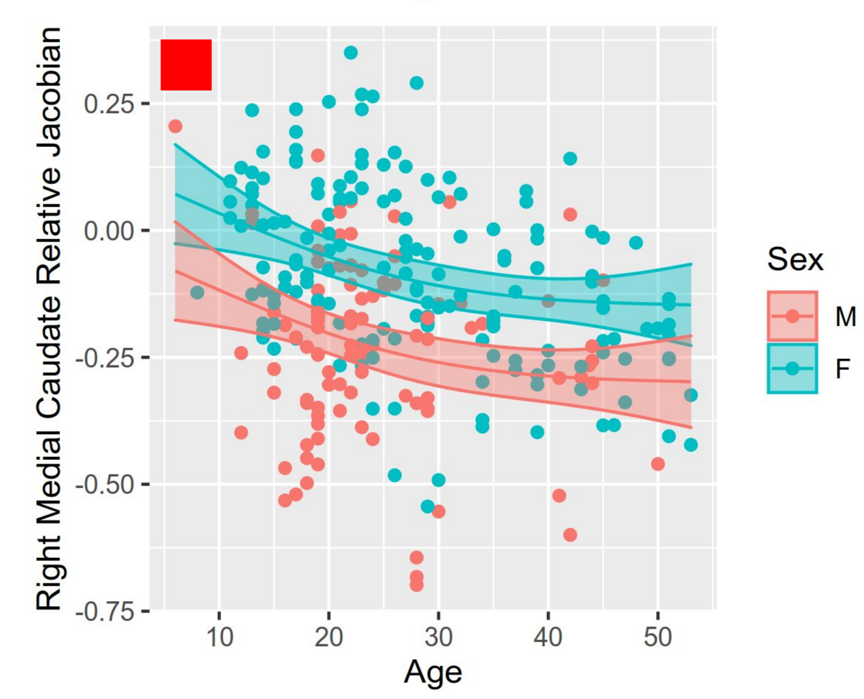

Figure 5: Regions with significant sex differences via t-value maps for female vs male using relative Jacobians. Colour thresholded 5% to 1% FDR.

While global absolute volume differences between male and female chimpanzees are large, there is limited focal relative volume differences.

Of note is the medial caudate which is larger (plotted curve), and anterior cerebellar white matter, which is smaller (not shown).

References

[1] Aging of the cerebral cortex differs between humans and chimpanzees. Sherwood CC, Gordon AD, Allen JS, Phillips KA, Erwin JM, Hof PR, Hopkins WD. Proc Natl Acad Sci U S A. 2011 Aug 9;108(32):13029-34. doi: 10.1073/pnas.1016709108.

[2] Avants, B.B., Tustison, N.J., Song, G., Cook, P.A., Klein, A., Gee, J.C., 2011. A reproducible evaluation of ANTs similarity metric performance in brain image registration. Neuroimage 54, 2033–2044. https://doi.org/10.1016/j.neuroimage.2010.09.025

[3] Douglas Bates, Martin Maechler, Ben Bolker, Steve Walker (2015). Fitting Linear Mixed-Effects Models Using lme4. Journal of Statistical Software, 67(1), 1-48. doi:10.18637/jss.v067.i01.

[4] Kuznetsova A, Brockhoff PB, Christensen RHB (2017). “lmerTest Package: Tests in Linear Mixed Effects Models.” Journal of Statistical Software, 82(13), 1-26. Doi: 10.18637/jss.v082.i13 (URL: https://doi.org/10.18637/jss.v082.i13).

[5] Lerch J, Hammill C, van Eede M, Cassel D (2017). RMINC: Statistical Tools for Medical Imaging NetCDF (MINC) Files. R package version 1.5.2.3, <URL: http://mouse-imaging-centre.github.io/RMINC>.

[6] Benjamini, Y., Hochberg, Y., 1995. Controlling the False Discovery Rate: A Practical and Powerful Approach to Multiple Testing. J. R. Stat. Soc. Series B Stat. Methodol. 57, 289–300.

Conclusions

Our closest relative, the Chimpanzee offers much insight into our evolutionary origins, and the brain structure differentiation and specialization we have undergone since our last common ancestor. Here we have presented a small look into the results of an extensive set of modelling of the changes of brain structure for both sexes across the natural lifespan. Both age and sexual differentiation patterns will be in the future compared to large-scale human data, and subject-wise variability examined, to investigate where brain structure development has been modified by evolution.